CHEMISTRY OF MATERIALS

Article

pubs.acs.org/cm

High-Density Lipoprotein-like Magnetic Nanostructures (HDL-MNS): Theranostic Agents for Cardiovascular Disease

Vikas Nandwana,[†,‡] Soo-Ryoon Ryoo,[†,‡] Shanthi Kanthala,[†,‡] Kaylin M. McMahon,[‡,§] Jonathan S. Rink,[‡,§] Yue Li,[#] Subbu S. Venkatraman,[¶] C. Shad Thaxton,[‡,§] and Vinayak P. Dravid*[,†,‡,#]

[†]Department of Materials Science & Engineering, Northwestern University, Evanston, Illinois 60208, United States

[‡]International Institute for Nanotechnology (IIN), Northwestern University, Evanston, Illinois 60208, United States

[§]Feinberg School of Medicine, Department of Urology, Northwestern University, Chicago, Illinois 60611, United States

[#]Applied Physics Program, Northwestern University, Evanston, Illinois 60208, United States

[¶]School of Materials Science and Engineering, Nanyang Technological University, Singapore 639798

Supporting Information

ABSTRACT: We report the development of potential theranostic agents for cardiovascular disease that are based on high-density lipoprotein-like magnetic nanostructures (HDL-MNS). The HDL-MNS offer prospects for diagnosis via noninvasive magnetic resonance imaging for anatomic detection and also serve as effective cholesterol efflux agents to address atherosclerotic vascular lesions. The HDL-MNS are synthesized by adding phospholipids and the HDL-defining apolipoprotein A1 to the surface of magnetic nanostructures (MNS) to mimic some aspects of natural HDL particles. From a diagnostic perspective, HDL-MNS show a 5 times higher contrast (r_2 relaxivity up to 383 mM^{-1} s^{-1}) in magnetic resonance imaging (MRI) than commercially available T_2 MRI contrast agents (e.g., Ferumoxytol). Internalization of HDL-MNS by macrophage cells was confirmed by transmission electron microscopy (TEM), energy dispersive X-ray spectroscopy (EDX), inductive-coupled plasma mass spectrometry (ICP-MS), and successfully imaged via MRI. Also, the HDL-MNS particles show capacity to induce cholesterol efflux (~4.8%) from macrophage cells comparable to natural HDL (~4.7%), providing a pathway to prevent and treat cardiovascular disease via reverse cholesterol transport. The ability to image macrophage cells that have internalized HDL-MNS along with the cholesterol efflux capacity demonstrates the potential of the HDL-MNS particles as theranostic agents.

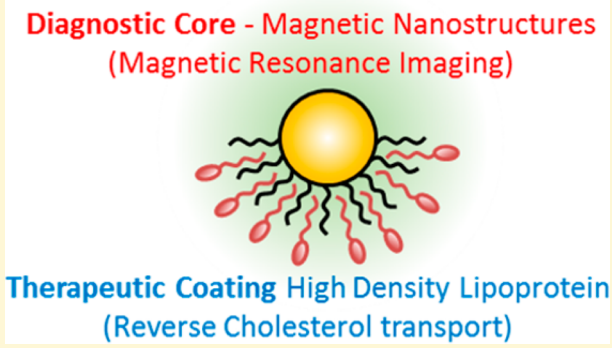

INTRODUCTION

Heart disease is one of the leading causes of death in the world due to a lack of early detection and targeted therapy.[1] The mechanism largely responsible for the development of cardiovascular disease is atherosclerosis, wherein excess fat and cholesterol in the bloodstream accumulates in macrophages, resulting in the formation of plaques in the walls of coronary arteries.[2] Plaque rupture results in rapid clot formation which partially or completely obstructs the flow of oxygen rich blood to the heart, resulting in a heart attack.[3] Targeted therapy is necessary to control plaque progression, especially those plaques that are vulnerable to rupture, whereas imaging of the atherosclerotic lesion is essential to monitor plaque size and composition before and during therapy.[4,5] Development of a "theranostic agent" that can diagnose atherosclerotic plaques at an early stage while providing therapeutic function by reducing plaque size is of great interest.

High-density lipoproteins (HDL), consisting of apolipoprotein A1 (apoA1) and phospholipids surrounding a core of cholesteryl esters and triglycerides, are responsible for effluxing cholesterol from lipid-laden macrophages in the periphery and transporting it back to the liver, in the atheroprotective process called reverse cholesterol transport (RCT).[6] RCT is thought to be a key mechanism protecting against cardiovascular disease. Increasing the levels of HDL provides a promising therapeutic approach to prevent and potentially reverse atherosclerosis by augmenting RCT.[7−9] However, most of the drugs to increase HDL levels, as well as administration of apoA1 (reg or Milano) have not demonstrated great results in clinical trials. Thaxton and co-workers have reported on a bioinspired HDL nanoconstruct with a gold nanoparticle core template as a potential therapeutic agent due to its capability to bind and efflux cholesterol from target cells.[10−12] Fayad, Fisher, and co-workers reported synthetic HDL type nanoparticles composed of Gd-chelates and phospholipids to image and characterize atherosclerotic plaque via magnetic resonance imaging

Received: December 18, 2016
Revised: February 24, 2017
Published: February 24, 2017

DOI: 10.1021/acs.chemmater.6b05357
Chem. Mater. 2017, 29, 2276−2282

(MRI).[13−17] MRI is a preferred method of noninvasive imaging due to its high spatial resolution, excellent soft tissue contrast and lack of ionizing radiation, such as X-rays.[18,19] Mulder, Fayad, and co-workers reported HDL mimicking nanoparticles capable to be imaged by computed tomography, magnetic resonance, and fluorescence imaging by incorporation of gold nanoparticles, iron oxide (FeO) nanoparticles, and quantum dots, respectively.[20,21] Synthetic HDL mimic composed of PLGA, phospholipids, and quantum dots (QDs) or fluorophores were reported for detection of atherosclerotic plaque via optical imaging.[22,23] Recently, Zheng et al.[24] have shown the ability of natural prebeta HDL mimic (CER-001) to target and visualize the plaques in atherosclerotic patients via PET/CT and contrast enhanced MRI as well as to enhance plasma cholesterol efflux capacity in patients. However, all the reported nanoconstructs either demonstrate diagnostic function with very low (or no) cholesterol efflux capacity or lack imaging capability. Moreover, recently cellular toxicity from Cd based quantum dots and nephrotoxicity from Gd based MR agent have been reported.[25,26] There have been few reports of theranostic nanoparticles that target plaque and show diagnostic and/or therapeutic function but their formulation does not mimic HDL.[27,28] Hence, there are compelling opportunities in the design of HDL-mimics that can provide imaging as well as therapeutic function.

Herein we report the development of HDL-mimic theranostic agents for cardiovascular disease that may be capable of precise anatomic detection as well as early treatment of cholesterol-rich atherosclerotic lesions. High-density lipoprotein-like magnetic nanostructures (HDL-MNS) were synthesized by coating phospholipids and apoA1 onto magnetic nanostructures (MNS) to mimic the surface composition of natural HDL (Scheme 1). The MNS are composed of Fe_3O_4 nanoparticles, which are among the most common, biocompatible T_2 contrast agents for MRI. From the diagnostic perspective, the HDL-MNS particles act as magnetic resonance imaging (MRI) probes that can target and localize to macrophages, the key cell type in atherosclerotic lesions. The HDL-MNS particles display 5 times higher MR contrast (r_2 relaxivity up to 383 mM^{-1} s^{-1}) than a commercially available T_2 MRI contrast agent (Ferumoxytol). From the therapeutic perspective, the HDL-MNS particles show higher capacity to induce cholesterol efflux (∼4.8%) from macrophage cells with comparison made to natural HDL (∼4.7%). The internalization of HDL-MNS particles by macrophage cells was confirmed by TEM/EDS, ICP-MS, and later successfully imaged using MRI. Hence, the HDL-MNS provide a pathway to potentially, detect, prevent, and treat cardiovascular disease.

Scheme 1. Approach 1 To Synthesize HDL-MNS A Particles Where Oleic Acid Coated Hydrophobic MNS Were First Coated with a Neutral Lipid 1,2-Dipalmitoyl-*sn*-glycero-3-phosphocholine (DPPC) and Later Coated with Apolipoprotein A1 (apoA1); In Approach 2, Hydrophilic MNS Were First Coated with apoA1 and then Coated with DPPC, Resulting in HDL-MNS B Particles

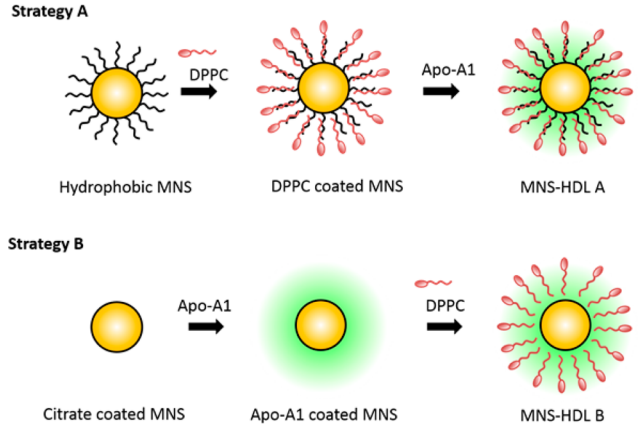

EXPERIMENTAL SECTION

Materials. DPPC and NBD-PC were purchased from Avanti Polar Lipids. The apoA1 was purchased from Meridian Life Science. Alexa Fluor 488 Protein Labeling Kit was obtained from Thermo Fisher Scientific Inc. Cell culture supplies were purchased from Invitrogen (Carlsbad, CA). [1,2-^{3}H(N)]-Cholesterol (^{3}H-cholesterol) was obtained from PerkinElmer.

Synthesis of HDL-MNS. HDL-MNS particles were synthesized via two approaches. In the first approach, oleic acid coated hydrophobic MNS were dispersed in chloroform and incubated with neutral lipid 1,2-dipalmitoyl-*sn*-glycero-3-phosphocholine (DPPC, Avanti Polar Lipids, Inc.) dissolved in chloroform (25 mg/mL) for 30 min (weight ratio MNS:DPPC = 1:3). The chloroform was evaporated and water was added gradually. After sonication, DPPC coated MNS dispersed in water were obtained. Later, DPPC coated MNS were incubated with 5-fold molar excess apoA1 and dialyzed, resulting in HDL-MNS A particles (Scheme 1). In the second approach, the human apoA1 (1 mg/mL, Meridian Life Sciences) was incubated with 10-fold molar excess of 8 nm of citrate coated MNS dispersed in 10 mM sodium phosphate buffer (pH 7.8) for 4−6 h at room temperature. Next, DPPC dissolved in ethanol (1 mg/mL) was mixed with the apoA1-MNS solution in 20-fold molar excess and incubated for overnight with gentle agitation. To eliminate unbound protein and lipids, the solutions of HDL-MNS A and B were purified by dialysis using Prewetted Spectra/Por 6 Dialysis Tubing (molecular weight cutoff, 50 kDa, Spectrum Laboratories, Inc.) in 10 mM phosphate buffer. The HDL-MNS concentration was measured by ICP-MS (inductively coupled plasma mass spectrometry). Particle size distribution and ζ-potential of synthesized HDL mimic MNS were determined by Malvern Zetasizer Nano ZS90Malvern, USA).

apoA1 and Phospholipid Binding. To determine the number of apoA1 protein per HDL-MNS, fluorescently labeled apoA1 was prepared using Alexa Fluor 488 Protein Labeling Kit (Thermo Fisher Scientific Inc.) described in previous report.[10] The number of apoA1 per HDL-MNS was calculated by comparing the fluorescence from AF488-apoA1 HDL-MNS to the standard curve. The number of phospholipids per HDL-MNS was analyzed in a similar manner, using a commercially obtained fluorescently tagged lipid (NBD-PC).

Cell Culture. J774 cells were grown in RPMI-1640 medium containing 10% FBS and penicillin/streptomycin (100 units/mL and 100 μg/mL, respectively). The cells were cultured at 37 °C with 5% CO_2 atm and plated in T75 flasks with the aforementioned media.

Cholesterol Efflux Assay. J774 macrophage cells were used as murine cell culture model for cholesterol efflux to HDL-MNS. The cells were seeded at 15 × 10^4 cells per well in 24-well plate and cultured for 24 h. The next day, cells were washed with PBS and incubated with 1 μCi/mL [1,2-^{3}H(N)]-cholesterol for 24 h to label the intracellular pools of cholesterol. After media was removed and washing with serum-free media, cells were exposed to HDL-MNS for 4 h in fresh culture media. Serum HDL and purified apoA1 were incubated with the cells as positive controls, and lipidated MNS (L-MNS) and citrate coated MNS were used as negative controls for comparison. At the end of efflux, cell media were collected with vacuum filtration to remove floating cells and subjected to liquid scintillation counting.

Cholesterol Binding Experiments. The cholesterol binding to HDL-MNS was determined by using a fluorescent cholesterol analogue (NBD-cholesterol). The NBD-cholesterol solution was

DOI: 10.1021/acs.chemmater.6b05357
Chem. Mater. 2017, 29, 2276−2282

prepared in dimethylformamide (DMF) with varying concentrations. Fluorescence spectra of the solutions were measured after mixing 5 μL of NBD-cholesterol in DMF with 10 nM HDL-MNS in PBS and incubating for 20 min at room temperature. The solutions were excited at 473 nm and scanned from 500 to 600 nm in 1 nm increments with 1 s integration times. The fluorescence intensity of NBD-cholesterol solution without particles were used as control and subjected to subtract the background signal. The fluorescence signal of NBD-cholesterol was detected and increased at 550 nm upon cholesterol binding, making the binding isotherm. As previously reported,[10] equilibrium dissociation constants (K_d) were calculated by analyzing the binding curves with "one site total binding" function.

Circular Dichroism Analysis. The structures of free form and conjugated apoA1 on HDL mimic MNS under the same buffer condition (10 mM sodium phosphate buffer) were analyzed by a Jasco J-815 CD spectrophotometer (JASCO). The CD spectra of nanoconstructs were also subtracted from background CD of MNS (no apoA1) in the same buffer.

MTS Assay for Cell Viability Test. J774 cells were plated at 2×10^4 cells per well in a 96-well plate with 70−80% confluency. MTS (3-(4,5-dimethylthiazol-2-yl)-5-(3-carboxymethoxyphenyl)-2-(4-sulfophenyl)-2H-tetrazolium) assay was used to quantify the cell viability according to the protocol provided by the manufacturer (CellTiter 96 Aqueous One Solution Cell Proliferation Assay; Promega). Cells were incubated with HDL-MNS at concentrations ranging from 0 to 350 μM for 24 h at 37 °C. Following treatment, cells were rinsed with PBS buffer briefly and further incubated with 20 μL of MTS stock solution into each well for an additional 1−4 h at 37 °C. The optical densities were recorded at 490 nm, and background absorbance at 700 nm was subtracted.

Measurement of r_2 Relaxivity. The T_2 relaxation times of HDL-MNS in solution were measured at 37 °C using a Bruker mq60 NMR analyzer (1.4 T, 60 MHz) equipped with Minispec V2.51 Rev.00/NT software (Billerica, MA). T_2 relaxation times were measured using a simple spin echo (SE, t2_co_mb).

MR Imaging of Cell Pellets. J774 cells were plated at 8×10^6 cells per well in a T75 flask with 70−80% confluency 1 day prior to particle treatment. Cells were cultured in various concentrations (0.1, 0.3, 1, and 3 μg/mL) of HDL-MNS and Ferumoxytol (commercially available and FDA-approved iron product for MR imaging) for 24 h. Untreated cells were used a control. Cell pellets were collected and placed in straws without bubble. After arranged, the cell pellets were imaged using 7 T Bruker Biospin MRI (Bruker Biospin, Billerica, MA).

Statistical Analysis. The unpaired two tailed student's t test from GraphPad Prism software (La Jolla, CA, USA) was used to analyze data of cholesterol efflux test and cell viability assay. Statistical significance was considered for significant for $P \leq 0.05$.

RESULTS AND DISCUSSION

Synthesis and Characterization of HDL-MNS. HDL-MNS particles were synthesized via two approaches. In the first approach, hydrophobic MNS were coated with DPPC and followed by apoA1, and are referred to as HDL-MNS A (Scheme 1). In the second approach, hydrophilic MNS were first incubated with apoA1 followed by coating with DPPC, termed HDL-MNS B (Figure 1). The particle size, hydrodynamic diameter, and ζ-potential are shown in Figure 1. Both HDL-MNS particles showed average hydrodynamic diameter in the range of 80−100 nm. To determine the number of apoA1 and phospholipid per HDL-MNS respectively, fluorescently labeled apoA1 and phospholipids were utilized. Quantification of apoA1 associated with HDL-MNS was done using Alexa Fluor 488-labeled protein. Alexa Fluor 488 labeling was performed according to the manufacturer's protocol (Life Technologies, Carlsbad, CA, USA), and purified by column chromatography. The ζ-potential were found in the range of −25 to −30 mV for HDL-MNS A and −14 to −17 mV for

(a)

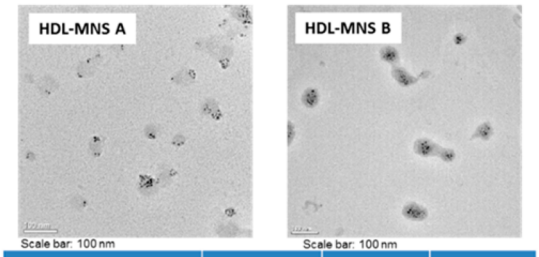

(b)

	Natural HDL**	HDL-MNS A	HDL-MNS B
Hydrodynamic Size (nm)	7 ~ 13	80 ~ 100	80 ~ 100
Number of Apo A1	2 ~ 4	3.2	2.5
Number of PL	160	1280	148
% of α-helicity of Apo A1	~ 67	~ 66	~ 84
Zeta Potential (mV)	X	-25 ~ -30	-14 ~ -17

Figure 1. Characterization data for HDL-MNS A and B particles. (a) Transmission electron microscopy (TEM) images and (b) hydrodynamic diameter, number of HDL component, the percentage of α-helicity, and ζ-potential analysis.

HDL-MNS B. The difference in ζ-potential was found due to the different number of apoA1 per HDL-MNS particle because apoA1 is composed of a negatively charged hydrophilic domain.[29]

The concentration and degree of labeling was determined using absorbance measured at 280 and 494 nm. The protein content (molar ratio) of the particles was calculated from the intensity of fluorescence after dialyzing the HDL-MNS.[10] As compared the fluorescence signal of HDL-MNS to the standard curve obtained from the known concentration of fluorescence labeled protein, 2.5−3.2 apoA1 were found per MNS on average for both HDL-MNS particles. The number of phospholipids on MNS was analyzed with similar experiments using commercially obtained fluorescently tagged phospholipid (NBD-PC).[10] From the fluorescence intensity, approximately 1280 molecules of lipid per MNS was found for HDL-MNS A whereas the number was 148 for HDL-MNS B. Circular dichroism was used to characterize the secondary structure of apoA1 to confirm its cholesterol efflux ability (Figure S1). Lipid-free apoA1 was used as a control. The similar α-helicity of lipid-free apoA1 and apoA1 on HDL-MNS suggested that the secondary structure of apoA1 in HDL-MNS was well preserved, a key criterion for the cholesterol efflux process.

r_2 Relaxivity Measurement of HDL-MNS. The MNS used in the study have core size of 8 nm that shows superparamagnetic behavior.[30,31] To determine the contrast enhancement effect, r_2 relaxivity of HDL-MNS of successive dilutions in water was measured at 1.4 T with a frequency of 60 MHz. Significantly high r_2 relaxivity values (340 and 383.8 mM^{-1} s^{-1} for HDL-MNS A and B, respectively) were obtained, ~5 times higher than that for commercially available T_2 contrast agent Ferumoxytol (80 mM^{-1} s^{-1}), as shown in Figure 2.[32] The higher relaxivity could be due to the multiple number of MNS present in the cluster form in the HDL-MNS particle. It is well-known that nanoclusters of MNS demonstrate higher r_2 relaxivity than isolated MNS due to synergistic magnetism produced by clusters.[33] These high numbers indicate the MR signal generated through the HDL-MNS particles can be 5 times stronger than Ferumoxytol. In other words, 5 times lower administration dosages of HDL-MNS particles may be used for the same MR signal as Ferumoxytol.

DOI: 10.1021/acs.chemmater.6b05357
Chem. Mater. 2017, 29, 2276−2282

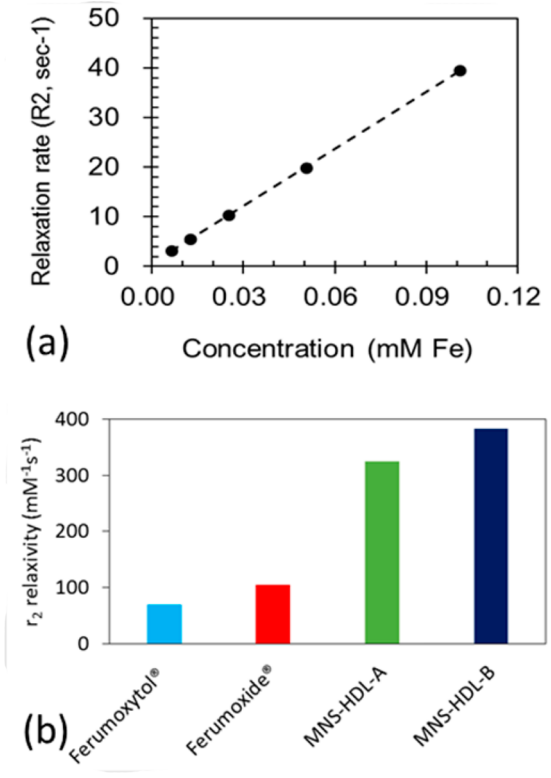

Figure 2. (a) r_2 relaxivity plot of HDL-MNS B particles measured at 1.4 T. (b) Comparison of r_2 values of HDL-MNS A and B with commercially available contrast agent; Ferumoxytol, and Ferumoxide.

Analysis of Cholesterol Binding in Solution by HDL-MNS. To investigate the potential therapeutic function of HDL-MNS, we quantified the ability of the HDL-MNS nanoconstructs to bind the fluorescently labeled cholesterol analog NBD-cholesterol. NBD-cholesterol has minimal fluorescence in polar environment but high fluorescence in nonpolar environment. When NBD-cholesterol binds to HDL and is incorporated into its lipid membrane, its fluorescence signal increases, which directly correlates with concentration of NBD-cholesterol bound. A cholesterol binding isotherm was plotted from normalized fluorescence intensities and the dissociation constant (K_d) for NBD-cholesterol binding to HDL-MNS A and B was found to be 331.3 and 69.9 nM, indicating very high binding affinity between HDL-MNS and cholesterol (Figure S2). There have not been any reports regarding K_d of natural HDL for comparison. However, the K_d values of HDL-MNS were very similar to the K_d values of HDL-Au nanoparticles (60−650 nM) reported by Thaxton and co-workers.[12]

Determination of Cholesterol Efflux by HDL-MNS. The atheroprotective action of HDL can be mainly attributed to its ability to efflux cholesterol from lipid-laden macrophages, termed foam cells, in atherosclerotic plaques.[6] The J774 murine macrophage cell was used to determine the cholesterol efflux capacity of the HDL-MNS, using standard protocols. After overnight labeling of the cells with [^{3}H] cholesterol, ABCA1 was induced using cAMP. The cholesterol acceptors HDL-MNS, serum HDL, or apoA1 were incubated with the cells for 4 h and the radioactivity of the culture media measured by a liquid scintillation counter. Percent efflux was calculated as described previously.[10] The cholesterol efflux values from HDL-MNS A and B were found to be 4.8% and 2.4%, respectively. The efflux values from HDL-MNS A were higher than that from apoA1 protein alone, and comparable with natural HDL (4.7%), indicating the potential atheroprotective nature of HDL-MNS particles similar as natural HDL (Figure 3).[12] Lipidated MNS (L-MNS), synthesized by adding the

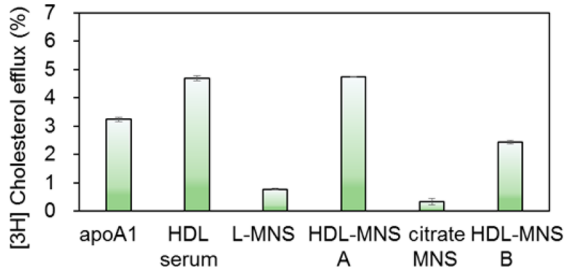

Figure 3. Cholesterol efflux from J774 macrophage cell lines by HDL-MNS. HDL-MNS show high percent efflux compared to apoA1 and serum HDL treated at similar conditions. Lipidated-MNS and citrate MNS samples did not induce efflux indicating the specificity.

phospholipid DPPC to MNS in the absence of apoA1, and citrate-stabilized MNS did not induce efflux, indicating that apoA1 is essential for the cholesterol efflux to HDL-MNS.

Biocompatibility of HDL-MNS. The cytotoxicity of HDL-MNS was evaluated using an MTS (3-(4,5-dimethylthiazol-2-yl)-5-(3-carboxymethoxyphenyl)-2-(4-sulfo-phenyl)-2H-tetrazolium) assay on J774 cells (Figure 4). It is a colorimetric assay

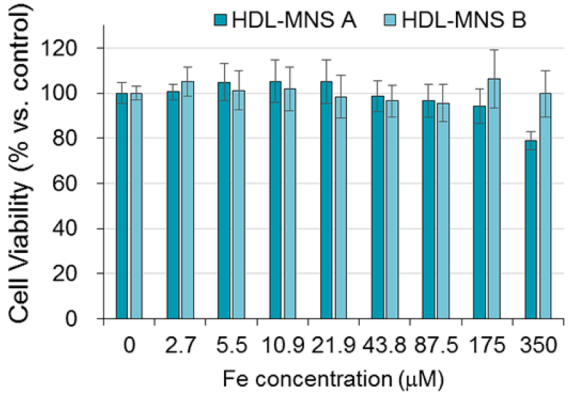

Figure 4. Cell viability of HDL-MNS A and B in J774 murine macrophage cell lines with the range of effective working concentrations up to 350 μM [Fe] (incubation time: 24 h).

that determines the quantity of formazan end product, which is directly proportional to the number of viable cells. The ratio of absorbance in treatment wells to control was used to report percent viability of cells. From the cell viability data of macrophage cells, HDL-MNS were nontoxic up to 350 μM iron concentration and can be used further for in vitro and in vivo studies up to these concentrations.

In Vitro Localization Study of HDL-MNS. From the diagnostic perspective, HDL-MNS internalized by the macrophage cells can potentially be used to image atherosclerotic plaques via MRI. The cellular uptake was confirmed by TEM/EDS of the HDL-MNS particles incubated with J774 cells for 24 h (Figure 5). Cells were fixed primarily with 2.5% glutaraldehyde and 2% formaldehyde mixture. A postfixation was done with osmium tetroxide. After dehydration by a series of ethanol washes, the sample is embedded in resin.

DOI: 10.1021/acs.chemmater.6b05357
Chem. Mater. 2017, 29, 2276−2282

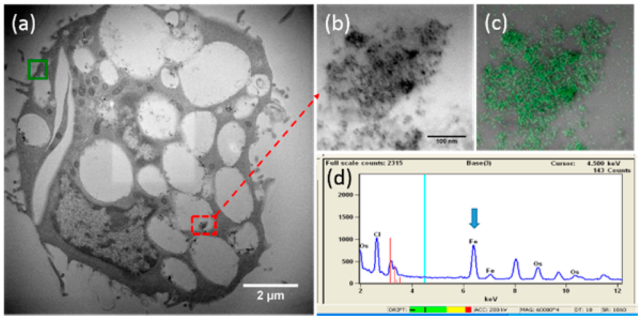

Figure 5. TEM (transmission electron microscopy) and EDS (energy dispersive spectrum) of HDL-MNS A taken up by J774 macrophage cells. (a) Dark-field TEM low magnification TEM image. (b) High-magnification image, (c) corresponding Fe-map (green), and (d) EDS spectra confirm uniform distribution of HDL-MNS particles into J774 cells.

Ultramicrotome sections were placed on a TEM grid and images were taken. It was observed that the particles were uptaken by endocytosis and localized in vesicular structures of the cytoplasmic regions. EDS spectral and point scans show the presence of iron confirming the presence of particles inside cells. This result is different than the initial reports that suggest HDL removes excess cholesterol from periphery of macrophages via SR-B1 receptors and delivers it to the liver.[34] However, there have been several reports suggesting other mechanism of cholesterol efflux from macrophages in which cholesterol is transported to apoA1 by ABCA1 or by retro-endocytosis via SR-B1 or ABCG1.[35] The retro-endocytosis involves endocytosis of HDL into the macrophage cells followed by their resecretion after taking up cholesterol.[36,37] In our case, internalization of HDL-MNS into the J774 macrophage cells suggests the possible mechanism of cholesterol efflux to be retro-endocytosis.

In Vitro MR Imaging of HDL-MNS. T_2-weighted MR images of HDL-MNS were taken after incubation for 24 h in J774 cells. HDL-MNS nanoparticles and Ferumoxytol (commercial FDA-approved T_2 contrast agent) were incubated in J774 cells with various concentrations (0.1, 0.3, 1, and 3 μg/mL) (Figure 6a). Cell pellets were collected and then imaged using MR scan. Untreated cells were used as a control. T_2-weighted MR phantom images show a darker signal (decrease in T_2 relaxation time) with the increase of Fe concentration. The relaxation time drop for HDL-MNS particles was significantly higher than Ferumoxytol at similar iron concentrations, demonstrating higher contrast enhancement properties of HDL-MNS. Fe ion uptake per cell was calculated via ICP-MS of cell pellets used for MR imaging. Fe ion take up per cell increased with increasing Fe concentration of HDL-MNS samples treated with cells (Figure 6b). The internalization of HDL-MNS particles was found to be lower than that of Ferumoxytol. This could be due to the smaller hydrodynamic size of Ferumoxytol compared to HDL-MNS particles. A similar phenomenon has been reported previously where the smaller size of nanoparticle showed higher internalization in macrophages through scavenger-mediated phagocytosis compared to the larger sized nanoparticles.[38,39] Interestingly, even though more uptake was found in case of Ferumoxytol, the drop in T_2 relaxation time for HDL-MNS particles was significantly higher than that for Ferumoxytol at similar iron concentration, demonstrating higher contrast enhancement properties of HDL-MNS. It is important to note that the T_2

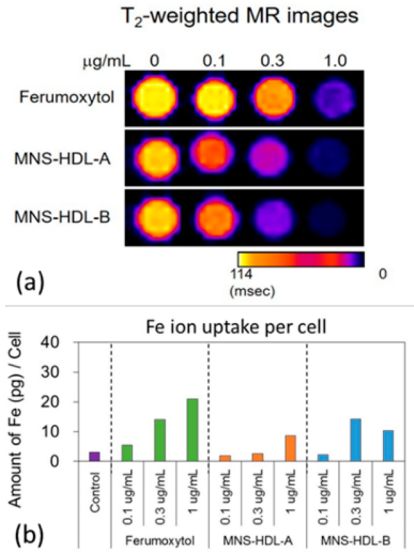

Figure 6. (a) T_2-weighted MR images of cell pellets after incubation for 24 h with HDL-MNS and Ferumoxytol (commercial FDA-approved T_2 contrast agent). T_2-weighted MR images shows darker signal (decrease in T_2 relaxation time) with the increase of Fe concentration. (b) Amount of Fe ion taken up per cell was measured via ICP-MS of cell pellets and show increase in Fe uptake with increasing Fe concentration. Interestingly, even though the more uptake was found in case of Ferumoxytol, the drop in T_2 relaxation time for HDL-MNS particles was significantly higher than that for Ferumoxytol at similar [Fe], demonstrating higher contrast enhancement properties of HDL-MNS.

signal of HDL-MNS in cells was found higher than in solution. There are several important factors that may contribute to the differences in signal intensities, namely the differing magnetic field strengths (1.4 T for solution vs 7 T for cells), pH (neutral for the solution vs slightly acidic in endosomes in cells), and potential clustering of HDL-MNS in endosomes in cells compared to being diffuse in solution.[40] It should be noted that the HDL-MNS signal was significantly higher than the Ferumoxytol in both solution and when applied to cells, clearly demonstrating the potential of HDL-MNS in comparison to currently available agents.

CONCLUSION

We have developed non-invasive theranostic agents for cardiovascular disease that may be capable of detecting as well as early treating macrophage- and cholesterol-rich atherosclerotic lesions. By mimicking some aspects of natural HDL particles present in the body, we have synthesized magnetic nanostructures functionalized with phospholipids and apoA1 protein, termed HDL-MNS. From the diagnostic perspective, the HDL-MNS particles show significantly higher MR contrast enhancement than FDA approved Fe_3O_4 based T_2 contrast agent Ferumoxytol. HDL-MNS particles internalization by macrophage cells was confirmed by TEM/EDS and ICP-MS, demonstrating the ability of HDL-MNS to label the relevant cell type in atherosclerotic plaques. Macrophages that had internalized HDL-MNS were then imaged using MR and data showed a higher T_2 contrast enhancement than commercial T_2 contrast agent, suggesting that the HDL-MNS imaging capabilities are on par with or better than the currently available agents. From the therapeutic perspective, HDL-MNS demonstrate functional and structural characteristics similar to

DOI: 10.1021/acs.chemmater.6b05357
Chem. Mater. 2017, 29, 2276−2282

natural HDL, namely their ability to bind and efflux cholesterol from cholesterol-rich macrophages. In vitro, HDL-MNS did not induce cytotoxicity in macrophages up to 350 μM iron, implying the nanoconstructs should not demonstrate toxicity when applied in an in vivo setting. Although we have demonstrated the ability of the HDL-MNS to target macrophages, modulate cholesterol flux, and be internalized within those cells, additional studies to test the targeting ability of HDL-MNS in an in vivo setting need to be conducted before moving forward with HDL-MNS as a potential theranostic therapy for cardiovascular disease. Finally, HDL-MNS particles provide further opportunities with regard to loading and delivering therapies, such as anti-inflammatory drugs, to macrophages located within established and developing atherosclerotic vascular lesions.

■ ASSOCIATED CONTENT

Supporting Information

The Supporting Information is available free of charge on the ACS Publications website at DOI: 10.1021/acs.chemmater.6b05357.

Additional analysis data: circular dichroism and cholesterol binding isotherm curve (PDF)

■ AUTHOR INFORMATION

Corresponding Author

*E-mail: v-dravid@northwestern.edu (V.P.D.).

ORCID

Vikas Nandwana: 0000-0002-7088-8813

Soo-Ryoon Ryoo: 0000-0003-2798-0443

Author Contributions

The manuscript was written through contributions of all authors. All authors have given approval to the final version of the manuscript.

Notes

The authors declare no competing financial interest.

■ ACKNOWLEDGMENTS

The authors gratefully acknowledges support from the NTU-NU Institute for NanoMedicine located at the International Institute for Nanotechnology, Northwestern University, USA and the Nanyang Technological University, Singapore. This work made use of the EPIC, Keck-II, and/or SPID facility(ies) of Northwestern University's NUANCE Center, which has received support from the Soft and Hybrid Nanotechnology Experimental (SHyNE) Resource (NSF ECCS-1542205); the MRSEC program (NSF DMR-1121262) at the Materials Research Center; the International Institute for Nanotechnology (IIN); the Keck Foundation; and the State of Illinois, through the IIN. Imaging work was performed at the Northwestern University Center for Advanced Molecular Imaging generously supported by NCI CCSG P30 CA060553 awarded to the Robert H. Lurie Comprehensive Cancer Center. J.S.R. is grateful for support from the NIH NHLBI Vascular Surgery Scientist Training Program (T32 HL094293).

■ REFERENCES

(1) Sanz, J.; Fayad, Z. A. Imaging of atherosclerotic cardiovascular disease. *Nature* **2008**, *451*, 953−957.

(2) Libby, P. Inflammation in atherosclerosis. *Nature* **2002**, *420*, 868−874.

(3) Libby, P.; Ridker, P. M.; Hansson, G. K. Progress and challenges in translating the biology of atherosclerosis. *Nature* **2011**, *473*, 317−325.

(4) Jayagopal, A.; Linton, M. F.; Fazio, S.; Haselton, F. R. Insights into Atherosclerosis Using Nanotechnology. *Curr. Atheroscler. Rep.* **2010**, *12*, 209−215.

(5) Lobatto, M. E.; Fuster, V.; Fayad, Z. A.; Mulder, W. J. M. Perspectives and opportunities for nanomedicine in the management of atherosclerosis. *Nat. Rev. Drug Discovery* **2011**, *10*, 835−852.

(6) Luscher, T. F.; Landmesser, U.; von Eckardstein, A.; Fogelman, A. M. High-Density Lipoprotein Vascular Protective Effects, Dysfunction, and Potential as Therapeutic Target. *Circ. Res.* **2014**, *114*, 171−182.

(7) Rosenson, R. S.; Brewer, H. B.; Ansell, B. J.; Barter, P.; Chapman, M. J.; Heinecke, J. W.; Kontush, A.; Tall, A. R.; Webb, N. R. Dysfunctional HDL and atherosclerotic cardiovascular disease. *Nat. Rev. Cardiol.* **2016**, *13*, 48−60.

(8) Navab, M.; Reddy, S. T.; Van Lenten, B. J.; Fogelman, A. M. HDL and cardiovascular disease: atherogenic and atheroprotective mechanisms. *Nat. Rev. Cardiol.* **2011**, *8*, 222−232.

(9) Damiano, M. G.; Mutharasan, R. K.; Tripathy, S.; McMahon, K. M.; Thaxton, C. S. Templated high density lipoprotein nanoparticles as potential therapies and for molecular delivery. *Adv. Drug Delivery Rev.* **2013**, *65*, 649−662.

(10) Thaxton, C. S.; Daniel, W. L.; Giljohann, D. A.; Thomas, A. D.; Mirkin, C. A. Templated Spherical High Density Lipoprotein Nanoparticles. *J. Am. Chem. Soc.* **2009**, *131*, 1384−1385.

(11) Luthi, A. J.; Lyssenko, N. N.; Quach, D.; McMahon, K. M.; Millar, J. S.; Vickers, K. C.; Rader, D. J.; Phillips, M. C.; Mirkin, C. A.; Thaxton, C. S. Robust passive and active efflux of cellular cholesterol to a designer functional mimic of high density lipoprotein. *J. Lipid Res.* **2015**, *56*, 972−985.

(12) Luthi, A. J.; Zhang, H.; Kim, D.; Giljohann, D. A.; Mirkin, C. A.; Thaxton, C. S. Tailoring of Biomimetic High-Density Lipoprotein Nanostructures Changes Cholesterol Binding and Efflux. *ACS Nano* **2012**, *6*, 276−285.

(13) Frias, J. C.; Ma, Y. Q.; Williams, K. J.; Fayad, Z. A.; Fisher, E. A. Properties of a versatile nanoparticle platform contrast agent to image and characterize atherosclerotic plaques by magnetic resonance imaging. *Nano Lett.* **2006**, *6*, 2220−2224.

(14) Frias, J. C.; Williams, K. J.; Fisher, E. A.; Fayad, Z. A. Recombinant HDL-like nanoparticles: A specific contrast agent for MRI of atherosclerotic plaques. *J. Am. Chem. Soc.* **2004**, *126*, 16316−16317.

(15) Cormode, D. P.; Briley-Saebo, K. C.; Mulder, W. J. M.; Aguinaldo, J. G. S.; Barazza, A.; Ma, Y. Q.; Fisher, E. A.; Fayad, Z. A. An ApoA-I mimetic peptide high-density-lipoprotein-based MRI contrast agent for atherosclerotic plaque composition detection. *Small* **2008**, *4*, 1437−1444.

(16) Cormode, D. P.; Chandrasekar, R.; Delshad, A.; Briley-Saebo, K. C.; Calcagno, C.; Barazza, A.; Mulder, W. J. M.; Fisher, E. A.; Fayad, Z. A. Comparison of Synthetic High Density Lipoprotein (HDL) Contrast Agents for MR Imaging of Atherosclerosis. *Bioconjugate Chem.* **2009**, *20*, 937−943.

(17) Briley-Saebo, K. C.; Geninatti-Crich, S.; Cormode, D. P.; Barazza, A.; Mulder, W. J. M.; Chen, W.; Giovenzana, G. B.; Fisher, E. A.; Aime, S.; Fayad, Z. A. High-Relaxivity Gadolinium-Modified High-Density Lipoproteins as Magnetic Resonance Imaging Contrast Agents. *J. Phys. Chem. B* **2009**, *113*, 6283−6289.

(18) Weissleder, R.; Pittet, M. J. Imaging in the era of molecular oncology. *Nature* **2008**, *452*, 580−589.

(19) Ehling, J.; Lammers, T.; Kiessling, F. Non-invasive imaging for studying anti-angiogenic therapy effects. *Thromb. Haemostasis* **2013**, *109*, 375−390.

(20) Cormode, D. P.; Skajaa, T.; van Schooneveld, M. M.; Koole, R.; Jarzyna, P.; Lobatto, M. E.; Calcagno, C.; Barazza, A.; Gordon, R. E.; Zanzonico, P.; Fisher, E. A.; Fayad, Z. A.; Mulder, W. J. M. Nanocrystal Core High-Density Lipoproteins: A Multimodality Contrast Agent Platform. *Nano Lett.* **2008**, *8*, 3715−3723.

(21) Skajaa, T.; Cormode, D. P.; Jarzyna, P. A.; Delshad, A.; Blachford, C.; Barazza, A.; Fisher, E. A.; Gordon, R. E.; Fayad, Z. A.; Mulder, W. J. M. The biological properties of iron oxide core high-density lipoprotein in experimental atherosclerosis. *Biomaterials* **2011**, *32*, 206−213.
(22) Marrache, S.; Dhar, S. Biodegradable synthetic high-density lipoprotein nanoparticles for atherosclerosis. *Proc. Natl. Acad. Sci. U. S. A.* **2013**, *110*, 9445−9450.
(23) Sanchez-Gaytan, B. L.; Fay, F.; Lobatto, M. E.; Tang, J.; Ouimet, M.; Kim, Y.; van der Staay, S. E. M.; van Rijs, S. M.; Priem, B.; Zhang, L. F.; Fisher, E. A.; Moore, K. J.; Langer, R.; Fayad, Z. A.; Mulder, W. J. M. HDL-Mimetic PLGA Nanoparticle To Target Atherosclerosis Plaque Macrophages. *Bioconjugate Chem.* **2015**, *26*, 443−451.
(24) Zheng, K. H.; van der Valk, F. M.; Smits, L. P.; Sandberg, M.; Dasseux, J. L.; Baron, R.; Barbaras, R.; Keyserling, C.; Coolen, B. F.; Nederveen, A. J.; Verberne, H. J.; Nell, T. E.; Vugts, D. J.; Duivenvoorden, R.; Fayad, Z. A.; Mulder, W. J.; van Dongen, G. A.; Stroes, E. S. HDL mimetic CER-001 targets atherosclerotic plaques in patients. *Atherosclerosis* **2016**, *251*, 381−388.
(25) Swaminathan, S. Gadolinium toxicity: Iron and ferroportin as central targets. *Magn. Reson. Imaging* **2016**, *34*, 1373−1376.
(26) Oh, E.; Liu, R.; Nel, A.; Gemill, K. B.; Bilal, M.; Cohen, Y.; Medintz, I. L. Meta-analysis of cellular toxicity for cadmium-containing quantum dots. *Nat. Nanotechnol.* **2016**, *11*, 479−486.
(27) Richardson, J. J.; Choy, M. Y.; Guo, J. L.; Liang, K.; Alt, K.; Ping, Y.; Cui, J. W.; Law, L. S.; Hagemeyer, C. E.; Caruso, F. Polymer Capsules for Plaque-Targeted In Vivo Delivery. *Adv. Mater.* **2016**, *28*, 7703−7707.
(28) McCarthy, J. R.; Jaffer, F. A.; Weissleder, R. A macrophage-targeted theranostic nanoparticle for biomedical applications. *Small* **2006**, *2*, 983−987.
(29) Sparks, D. L.; Lundkatz, S.; Phillips, M. C. The Charge and Structural Stability of Apolipoprotein-a-I in Discoidal and Spherical Recombinant High-Density-Lipoprotein Particles. *J. Biol. Chem.* **1992**, *267*, 25839−25847.
(30) Nandwana, V.; De, M.; Chu, S.; Jaiswal, M.; Rotz, M.; Meade, T. J.; Dravid, V. P.; Mirkin, C. A.; Meade, T. J.; Hurst Petrosko, S.; Stegh, A. H. Theranostic Magnetic Nanostructures (MNS) for Cancer. In *Nanotechnology-Based Precision Tools for the Detection and Treatment of Cancer*; Cancer Treatment and Research; Springer: Cham, 2015; Vol. *166*, pp 51−83, DOI: 10.1007/978-3-319-16555-4_3.
(31) Lee, N.; Yoo, D.; Ling, D.; Cho, M. H.; Hyeon, T.; Cheon, J. Iron Oxide Based Nanoparticles for Multimodal Imaging and Magnetoresponsive Therapy. *Chem. Rev.* **2015**, *115*, 10637−10689.
(32) Jung, C. W.; Jacobs, P. Physical and Chemical-Properties of Superparamagnetic Iron-Oxide Mr Contrast Agents - Ferumoxides, Ferumoxtran, Ferumoxsil. *Magn. Reson. Imaging* **1995**, *13*, 661−674.
(33) Roch, A.; Gossuin, Y.; Muller, R. N.; Gillis, P. Superparamagnetic colloid suspensions: Water magnetic relaxation and clustering. *J. Magn. Magn. Mater.* **2005**, *293*, 532−539.
(34) Krieger, M. Charting the fate of the "good cholesterol": Identification and characterization of the high-density lipoprotein receptor SR-BI. *Annu. Rev. Biochem.* **1999**, *68*, 523−558.
(35) Rohrl, C.; Stangl, H. HDL endocytosis and resecretion. *Biochim. Biophys. Acta, Mol. Cell Biol. Lipids* **2013**, *1831*, 1626−1633.
(36) Pagler, T. A.; Rhode, S.; Neuhofer, A.; Laggner, H.; Strobl, W.; Hinterndorfer, C.; Volf, I.; Pavelka, M.; Eckhardt, E. R. M.; van der Westhuyzen, D. R.; Schutz, G. J.; Stangl, H. SR-BI-mediated high density lipoprotein (HDL) endocytosis leads to HDL resecretion facilitating cholesterol efflux. *J. Biol. Chem.* **2006**, *281*, 11193−11204.
(37) Schmitz, G.; Robenek, H.; Lohmann, U.; Assmann, G. Interaction of High-Density Lipoproteins with Cholesteryl Ester-Laden Macrophages - Biochemical and Morphological Characterization of Cell-Surface Receptor-Binding, Endocytosis and Resecretion of High-Density Lipoproteins by Macrophages. *EMBO J.* **1985**, *4*, 613−622.
(38) Tsai, C. Y.; Lu, S. L.; Hu, C. W.; Yeh, C. S.; Lee, G. B.; Lei, H. Y. Size-Dependent Attenuation of TLR9 Signaling by Gold Nanoparticles in Macrophages. *J. Immunol.* **2012**, *188*, 68−76.
(39) Franca, A.; Aggarwal, P.; Barsov, E. V.; Kozlov, S. V.; Dobrovolskaia, M. A.; Gonzalez-Fernandez, A. Macrophage scavenger receptor A mediates the uptake of gold colloids by macrophages in vitro. *Nanomedicine* **2011**, *6*, 1175−1188.
(40) Takahashi, M.; Uematsu, H.; Hatabu, H. MR imaging at high magnetic fields. *Eur. J. Radiol.* **2003**, *46*, 45−52.

DOI: 10.1021/acs.chemmater.6b05357
Chem. Mater. 2017, 29, 2276−2282